Modeling of Sulfate Resistance of Flyash Blended Cement Concrete Materials

Barzin Mobasher[1], Aboozar Bonakdar[1] and Sudheen Anantharaman[1]

[1]Department of Civil and Environmental Engineering, Arizona State University, Tempe, Arizona, 85287-5306

KEYWORDS: sulfate attack, ettringite, cracking, expansion, diffusivity, concrete durability

ABSTRACT

Sulfate attack in concrete structures is among the major durability concerns in civil infrastructure systems. Proper modeling techniques can help us understand the influence of aggressive environments on the concrete performance, and improve the decision making process in every stage of construction and maintenance. Test procedures were developed to analytically and experimentally correlate the service condition of concrete with variable flyash levels subjected to external sulfate attack. Expansion tests were conducted according to ASTM C1012 using 1×1×11 in. specimens and the results were compared to the modified test using 0.4×0.4×1 in. specimens. Microstructure of the specimens were studied with Scanning Electron Microscopy (SEM) for compositional changes and formation of crack patterns due to sulfate exposure.

A simplified model is presented which used cement chemistry, concrete physics, and mechanics to develop a diffusion-reaction solution for predicting sulfate penetration, reaction, damage evolution and expansion, leading to degradation. A simplified approach is presented to compute the rate of degradation and expansion potential using a series solution approach. The model can address the interaction effects of various parameters using calibration data from various flyash compositions.

INTRODUCTION

Sulfate attack is the term used to describe a series of chemical reactions between sulfate ions and the components of hardened concrete, principally the cement paste, caused by exposure of concrete to sulfates and moisture. The chemistry of sulfate attack is complex and involves numerous overlapping reactions, mechanisms, and internal or external sources. Internal sulfate attack could be related to different forms of calcium sulfates which are added to clinker during cement grinding as a part of cement, also could be related to the aggregates or water with high SO_3 content. External sulfate

attack is generally related to natural sulfates of calcium, magnesium, sodium, and potassium present in soils or dissolved in ground water. [1]

A majority of the durability issues in concrete deal with the diffusion of one or several different ions into the material. However, due to the complexity of the different mechanisms involved, a single model predicting a universal response cannot be used. Very few durability models are currently applicable to external sulfate attack. Portland cement-based materials subjected to attack from sulfates may suffer from two types of damage: loss of strength of the matrix due to degradation of calcium-silicate-hydrate (C-S-H), and volumetric expansion due to formation of gypsum or ettringite that leads to cracking. Loss of strength has been linked to decalcification of the cement paste hydrates upon sulfate ingress, especially C-S-H, while cracking and expansion is attributed to formation of expansive compounds[2]. ASTM C1012 has been widely used by researchers to study the sulfate resistance of cement based materials by exposing 1×1×11 in. mortar specimens to 50 g/lit Na_2SO_4 or $MgSO_4$ solution[3]. However, there are deficiencies in this test method including lengthy measuring period (usually more than six months), insensitivity of the measurement tool to the progression of sulfate attack, the effect of curing (especially in the case of blended cements) and the effect of the pH change during the time in the solution [4, 5, 6]. Modifying the size of specimens could directly accelerate the sulfate attack without disturbing the degradation mechanism and would be more useful for a cement manufacturer to assess new hydraulic cements. In a recent study at NIST, Ferraris et al. used modified size specimens (0.4×0.4×1 in.) for studying the sulfate attack and showed that a reduction in testing time would be achieved by a factor of three to five. [5]

Efforts of modeling the durability due to external sulfate attack have received attention in the past decade[7]. An empirical relationship between ettringite formation and expansion is the basis for many models where the expansive strain is linearly related to the concentration of ettringite[8]. The general governing phenomena for the transfer of mass through concrete is modeled by means of conservation-type equations involving diffusion, convection, chemical reaction, and sorption. In the case of sulfates, some authors [9] assume that the process is controlled by reaction rather than diffusion, based on an empirical linear equation that links the depth of deterioration at a given time to the tri-calcium silicate (C_3A) content and the concentration of magnesium and/or sulfate in the original solutions. A solution of the diffusion equation with a term for first order chemical reaction was proposed to determine the sulfate concentration as a function of time and space. [10, 11] Similar to the recent work by the NIST group, the diffusion coefficient is represented as a function of the capillary porosity and varies with time since capillary pores fill up with the recently formed minerals[6]. Using micromechanics theory and the diffusion-reaction equation, a model that predicts the expansion of mortar bars has been developed for the 1-D case. [12]

EXPERIMENTAL PROGRAM

A comprehensive set of experiments to study the sulfate resistance of blended cement systems with as many as 10 different flyash compositions is currently being conducted.

The results of two flyash compositions in addition to the control specimen are discussed here. The chemical analysis and physical properties of the materials used are presented in Tables 1 and 2. Scanning Electron Microscopy (SEM) images of the two flyash particles including EDS spectrums for these materials are shown in Figures 1 and 2. As reported in Table 1, flyash composition labeled (FA1) with high SiO_2 content (58.7%) and low SO_3 content (0.2%) with an accepted LOI is classified according to ASTM C 618 as Class F. However, the composition labeled as (FA2) does not meet the classification of ASTM C 618 criteria, due to its high SO_3 content (10.1%) and high LOI, and is not suitable in a blended cement system. The cement used is a type I/II ordinary Portland cement with C_3A = 4.8%.

Flyash Code	**FA 1**	**FA 2**
SiO2	58.72	41.1
Al2O3	24.86	17.37
Fe2O3	4.94	3.45
Total S+A+F	88.52	61.92
CaO	4.56	19.8
MgO	1.57	1.33
SO3	0.21	10.12
L.O.I	0.25	4.18
Na2O	1.11	0.96
K2O	1.11	0.78
CaO / SiO2	0.08	0.48
Total Alka.	1.84	1.47
R Factor	-0.09	4.29
Moist.	0.03	0.27
P325	28.69	22.39
Reflect.	21.6	26.9
Spec. Grav.	2.08	2.22
Auto Clave	-0.03	-0.06
Poz. Cont. H2O	242	242
Poz. Test H2O	236	249
Poz. H2O% Req.	97.52	102.89
Poz. Day 7 Cont.	4370	4370
Poz. Day 7 Test	3990	4280
Poz. Day 7 Index	91.3	97.94
ASTM Check	CLASS F	Not Good
Sulfur Check	OK	Not Good
L.O.I Check	OK	Not Good
R Factor Check	OK	Not Good

Table 1. Chemical and physical properties of flyash used

Cement	**SiO2**	**Al2O3**	**Fe2O3**	**Total Alkali**	**CaO**	**MgO**	**SO3**	**L.O.I**	**Na2O**	**K2O**
type I-II	21.62	4.06	3.54	29.22	63.9	1.4	2.81	1.42	0.06	0.54

Free Lime	**C3S**	**C2S**	**C3A**	**C4AF**	**M325**	**Blaine**	**Reflect**	**Air**	**Auto Clave**
0.98	55.41	20.27	4.78	10.76	97.7	4260	29	9.4	-0.04

Table 2. Chemical and physical properties of cement used

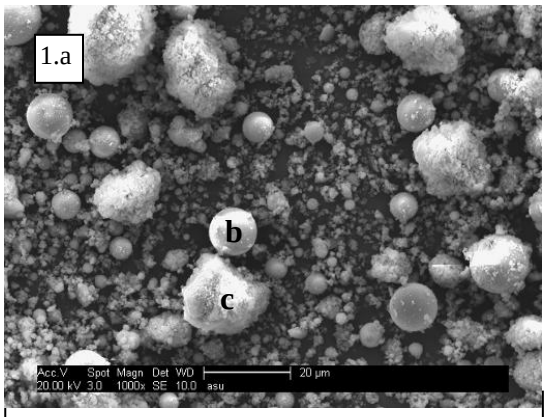

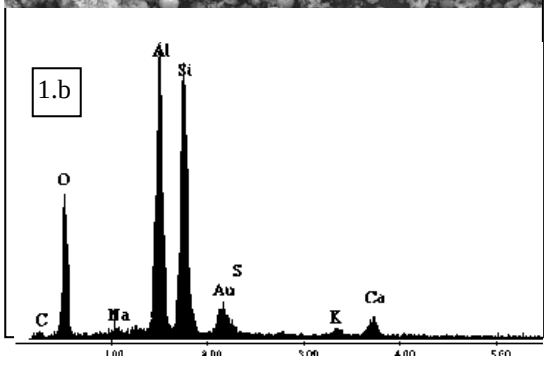

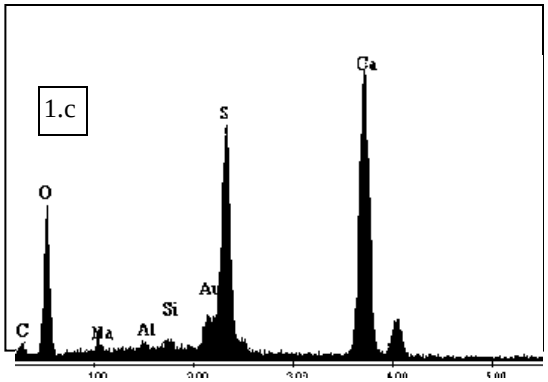

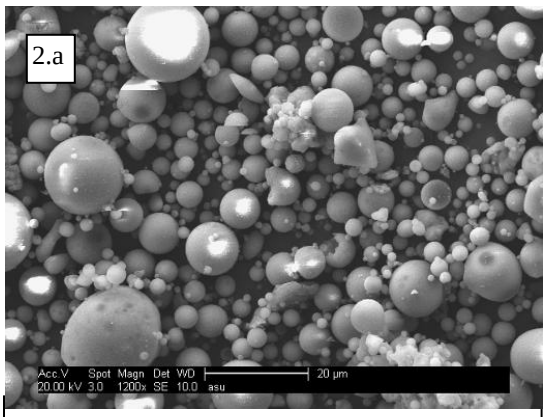

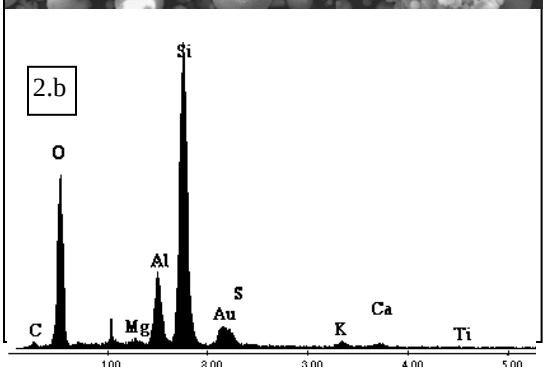

Figure 1.a: SEM image of flyash 2 (FA2) particles, magnification is 1000X.
Figure 1.b: EDS spectrum for particle b
Figure 1.c: EDS spectrum for particle c

Figure 2.a: SEM image of flyash 1 (FA1) particles, magnification is 1000X.
Figure 2.b: EDS spectrum for particle 2.b

Specimens were made using two different molds, the standard 1×1×11 in. molds according to ASTM C 1012, and the modified 0.4×0.4×4 in. in size shown in Figures 3-a and Figure 3-b. Mortar prisms were cast using w/cm = 0.6 and flyash-cement ratios of 0%, 20% and 30%, while paste specimens were made with w/cm = 0.4. Four specimens for the standard size and five specimens for the modified size were prepared and tested for each set of experiments. Specimens were cured in lime-saturated water for three days and then subjected to a sulfate solution containing 50 g/lit of Na_2SO_4 at room temperature. The pH of the solution was maintained between 6-8 by adding sulfuric acid every two weeks and by changing the solution every two months. Expansion measurement of the specimens was carried out periodically using separate digital comparators as illustrated in Figure 4. The average of all specimens for each set was obtained using a data processing algorithm to smooth and compute the average and

standard deviations of the data as shown in Figure 5. This average is then used for comparison of different sets of experiments and the model as well.

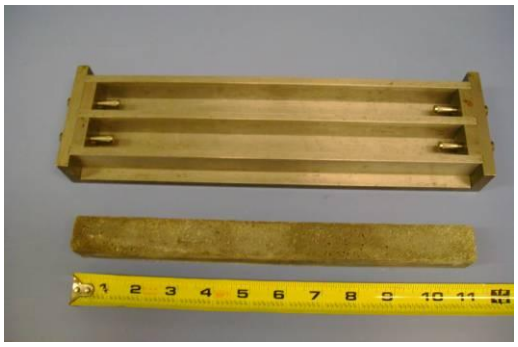

Figure 3.a. ASTM size 1×1×11 in. Molds and specimens

Figure 3-b. Modified size 0.4×0.4×4 in. Molds and specimens

Figure 4. Measurement of specimens using two separate digital gages for standard size (left) and modified size (right) specimens

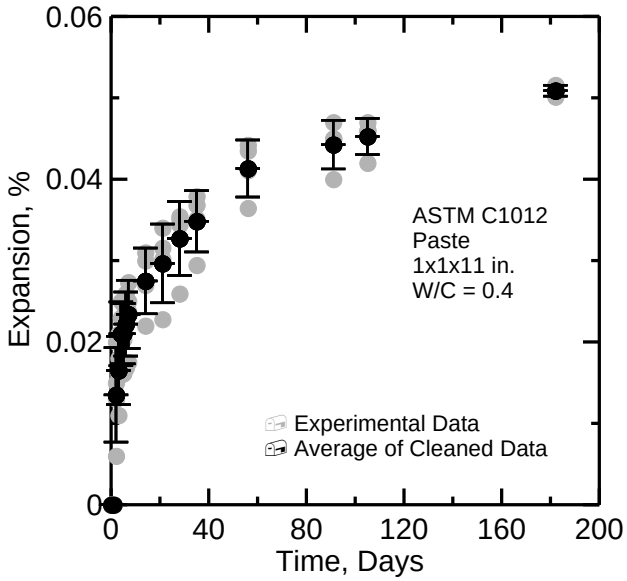

Figure 5. Average expansion of four/five specimens in each set of experiments is plotted using a clean-up program.

After six months of exposure, the expansion graphs of the standard and modified specimens are presented in Figures 6 and 7, respectively. Note that the maximum expansions in two graphs are considerably different (0.08% and 0.8% for Figure 6 and Figure 7, respectively), regardless of the sample composition. It is observed that replacing the cement with 20-30% Class F flyash (FA1) decreased the total expansion of standard size specimens by about 40% after 6 months of exposure. Note that at 20% substitution rate, FA2 (not classified) decreased the expansion by 20%, however, at 30% replacement level; this flyash increased the expansion by 60%. This major shift may be attributed to high SO_3 content. In the case of modified test, replacing 20% - 30% of cement by FA1 decreased the expansion by 20% after 6 months of exposure,

however, when using FA2 in cementitious system, significant expansion at about 180% is obtained.

Results of this study point out to the fact that small specimen's expansion data communicate the same level of results in a much faster time frame. It can be observed that on the average the results of 6 months exposure for the large ASTM specimens can be deduced only after about 60 days using the small sample sizes.

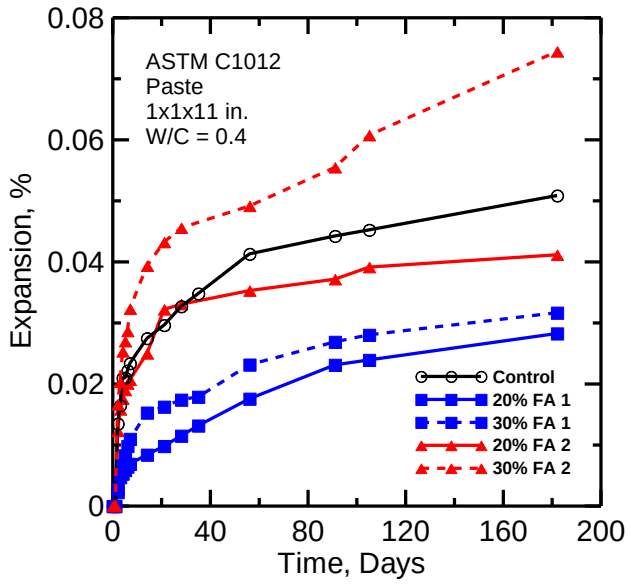

Figure 6. Six months expansion of standard size specimens for control and two flyash compositions

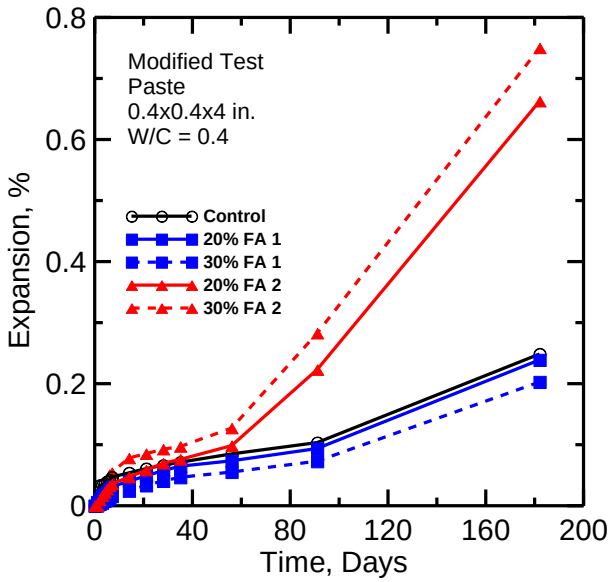

Figure 7. Six Months expansion of modified size specimens for control and two flyash compositions

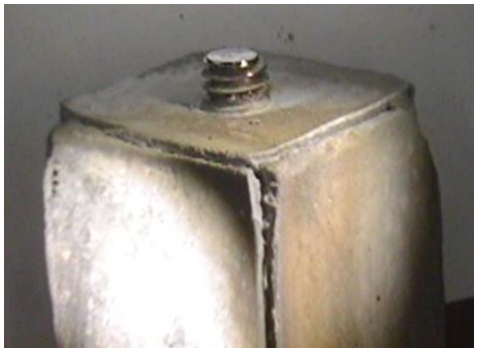

Figure 8. Diagonal racks along all edges for a standard size specimen, wider cracks are observed along the edges

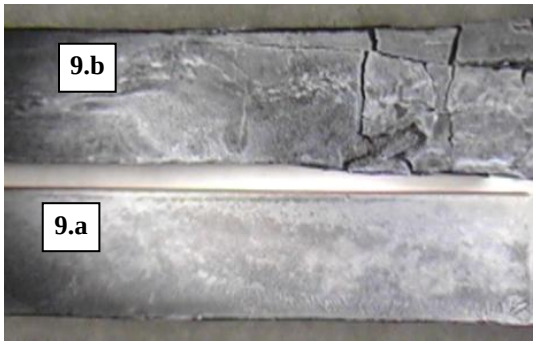

Figure 9. Modified size specimens (0.4x0.4x4") compared after 6 months of exposure to sodium sulfate solution. 9-a) FA2 and 9-b) FA1

Figure 8 shows the macroscopic cracks and degradation of FA1 specimens after six months of exposure to sulfate solution. Figures 9a and 9b show the comparison of FA1 and FA2 specimens after sulfate attack. It should be mentioned that all specimens for each set of experiments show a similar behavior in crack patterns along all edges. Peeling cracks along the longitudinal axis became visible which may be related to the ingress of sulfate ions into the material through the corners at a much faster rate. The sulfate concentration is expected to increase when reaching the outer sides and in the case of edges, the cracks are significantly wider. This is related to sulfate penetration from both edges.

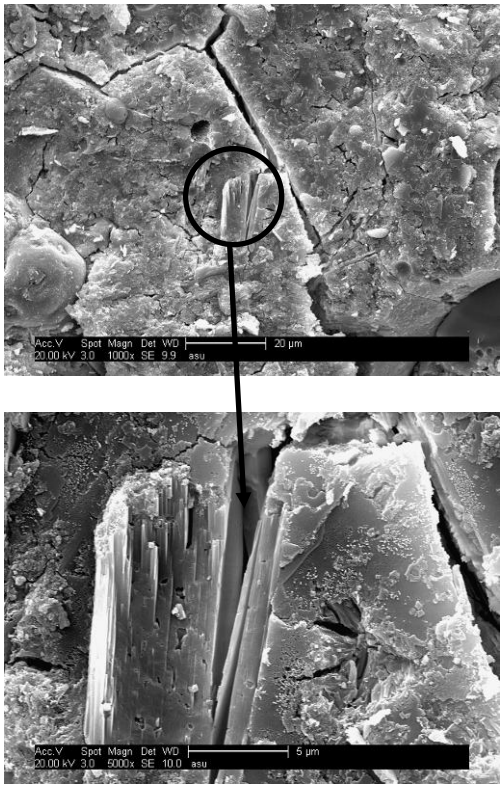

Figure 10. Formation of gypsum crystals near a crack in FA1 specimen exposed to sulfate attack

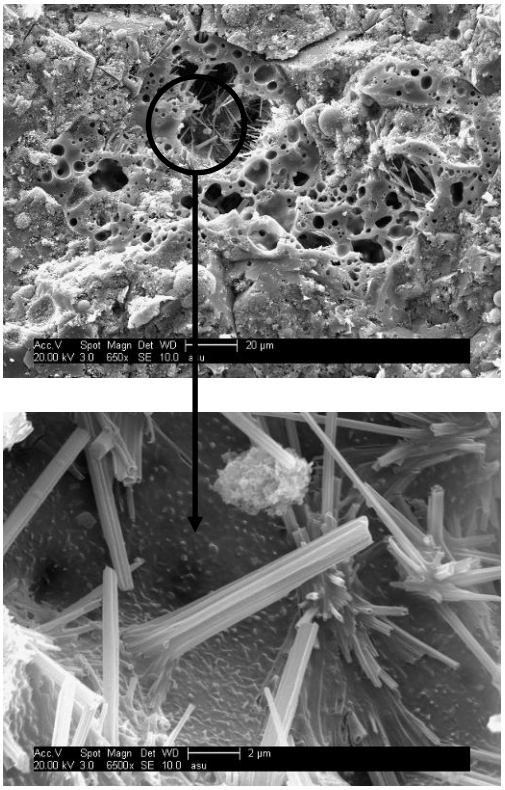

Figure 11. Formation of ettringite crystals in an air void in FA1 specimen exposed to sulfate

Scanning Electron Microscopy (SEM) was used to study the microstructure of the specimens after six months of exposure to sulfate solution. SEM images of FA1 samples are presented in Figures 10 and 11 showing the reaction products near or within cracks and air voids due to sulfate attack.

One can see the formation of gypsum crystals (calcium sulfate dihydrate, $CaSO_4.2H_2O$) near a crack, while ettringite crystals ($Ca_6Al_2(OH)_{12}.(SO_4)_3.26H_2O$, calcium aluminate trisulfate hydrate) are formed within the air void near the outer side of the specimen. Both gypsum and ettringite crystals were observed in as much as 75% of the air voids in

the control (C) and also flyash number 2 (FA2), however in the case of flyash number 1 (FA1), less than 50% of air voids were found to be filled with the reaction products. For the two flyash tested here, FA2 showed more deterioration with filled cracks and air voids.

MODELING

A chemo-mechanical mathematical model in simulating the response of concrete exposed to external sulfate attack has been developed using finite difference solution[13]. In the present approach, a simplified model based on a series based solution is presented[14]. The input parameters of this model include specimen size (length and width), chemical properties (C_3A and gypsum), mix design properties (w/cm, sand/cm, cement content), physical properties (degree of hydration, degree of reaction, diffusivity), mechanical properties (elastic modulus, tensile strength, residual stress) and exposure condition (sulfate concentration). The basic equation for the formation of ettringite from the Calcium Aluminate phase is represented as:

$$C_3A + 3C\bar{S}H_2 + 26H \longrightarrow C_6A\bar{S}_3H_{32} \quad (1)$$

In which C=CaO, S=SiO_2, A=Al_2O_3, H=H_2O, and $\bar{S}$=SO_3. C_3A is tricalcium aluminate, $C\bar{S}H_2$ is gypsum and $C_6A\bar{S}_3H_{32}$ is ettringite. Stoichiometric and molar volume relations are used to convert reacted sulfates to reacted aluminates, and ettringite formed. These reactions are lumped in a global sulfate phase-aluminate phase reaction as:

$$CA + q\bar{S} \longrightarrow C_6A\bar{S}_3H_{32} \quad (2)$$

The concentrations of the sulfate and the aluminate phases are represented as two parameters U and C respectively. It is assumed that there is sufficient amount of aluminates (C) present so that there is no depletion of this phase; one can therefore correlate the rate of reaction of the sulfates (U) with the aluminates phase into a single material constant, k, representing the rate of depletion of sulfates. The coupled differential equation for the penetration of sulfates and their reaction with the calcium aluminate phase is represented as a first order diffusion reaction equation and represented as the following:

$$\frac{\partial U(X,t)}{\partial T} = D\frac{\partial^2 U(X,t)}{\partial X^2} - kU(X,t)C(X,t) \quad (3)$$

$$\frac{\partial C(X,t)}{\partial T} = -\frac{kUC(t)}{q} \quad (4)$$

In equations 3 and 4, T represents the time, X is cross sectional location, D is the diffusivity of material and q is a constant representing the stoichiometric relationship between the available aluminates and the sulfates necessary for the reaction. Parameter “k” represents the rate of reaction of sulfates and aluminates. Equation 3 represents the rate of change of concentration of sulfates as a function of sulfate

diffusivity and Equation 4 represents the rate of reaction of aluminate phase and since aluminates are assumed to be stationary, no diffusion of this phase considered. Therefore, the change of aluminates is considered as a function of how fast it is reacting with sulfates based on the parameter k. By increasing k, the reaction takes place faster, and reducing it would have an effect of not allowing any depletion of calcium aluminates to take place.

The general solution for the two equations is presented by Tixier and Mobasher [13] . Equation 32 can be simplified as a single variable second order partial differential equation represented as Equation 4 and its series solution is represented as equation 6 as follows. Note that in this approach, it is assumed that the diffusivity remains constant and is not affected by the cracking. In this series solution, *n = m+1* and $\nu = D n^2 \pi^2 / L^2$ and U_0 is the initial sulfate concentration.

$$\frac{\partial U}{\partial T} = D \frac{\partial^2 U}{\partial X^2} - kU \tag{5}$$

$$\frac{U}{U_0} = 1 - \frac{4}{\pi} \sum_{m=0}^{\infty} \frac{1}{n(k+\nu)} \sin\left(\frac{n\pi X}{L}\right) \left[k + \nu \exp\left(T\left(k + \nu\right)\right)\right] \tag{6}$$

Computation of expansion in a sample using the simplified series solution algorithm is as follows. The solution for the series expansion of sulfate distribution is obtained as a function of time for a given diffusivity and rate of reaction as shown in figure 12. The baseline represents the case for the amount of sulfates that would have penetrated if there were no reactions. The average values of sulfates penetrated is obtained by integrating the U/U_0 values over the entire depth of the specimen. This level (average value of U/U_0) is multiplied by the initial sulfate concentration at the surface (ex. U_0= 0.35 moles/lit, as input) to find the concentration of reacted sulfates.

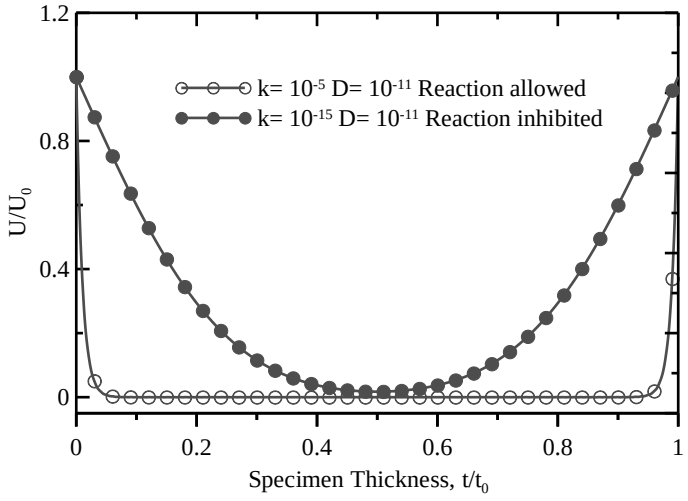

Figure 12. The sulfate penetration profile as a function of position [14]

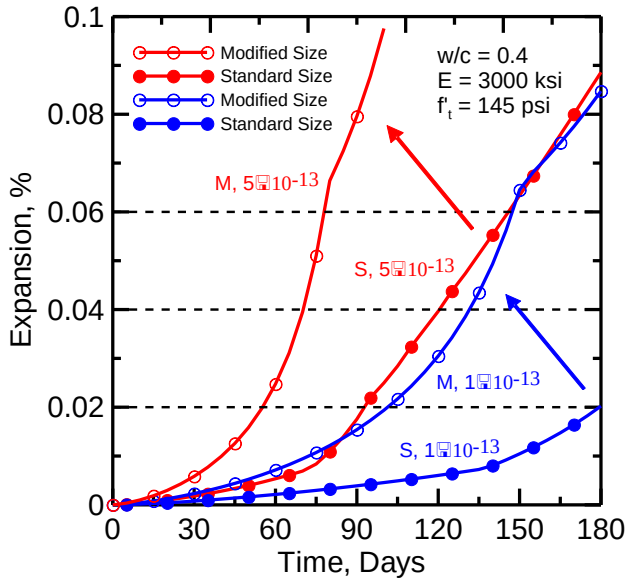

Figure 12. The effect of specimen size and diffusivity on the 6 month expansion of paste specimens predicted by the series solution model (M: modified, S: standard)

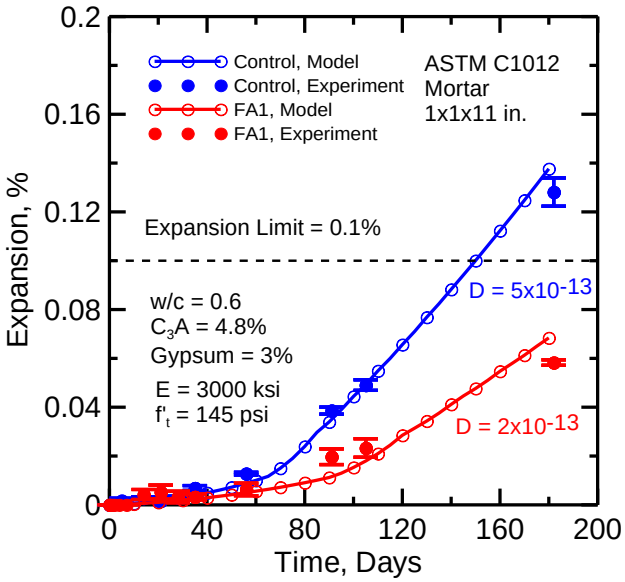

Figure 13. The comparison between control (C) and flyash (FA1) mortar specimens (standard size), measured via experiment (Exp.) and predicted via series solution model (Mod.)

One could use this simplified model for a parametric study to predict the expansion of mortar or paste specimens in accordance with different input parameters used, including specimen size, chemical parameters of materials, mix design properties, mechanical properties of hardened material and also the exposure conditions. Figure 13 shows the effect of specimen size as well as diffusivity of the material. It can be observed that using small size specimens could shorten the time required for specific levels of expansion shown by dotted lines compared to large specimens. It is also clear that the diffusivity could directly affect the expansion due to sulfate attack. In the case of blended cements, pozzolans decrease the diffusivity via improving the microstructure of the material. The blue lines show D = $1x10^{-13}$ while red lines represent D = $5x10^{-13}$. The arrows show the expansion change obtained from the modified size specimens.

Figure 13 shows the comparison of experimental results and the simplified model prediction for the six months expansion of mortar bars. The blue line with blank circles shows the model prediction for the control specimen with coefficient of diffusivity of $5x10^{-13}$ while the blue circles show the average value of experimental results along with the standard deviation bars. On the other hand, the red line with blank circles represents the prediction for the flyash 1 specimen with D = $2x10^{-13}$ and the red circles show the average value of this set of experimental results represented with the standard deviation bars. Although flyash is considered to improve the mechanical properties of hardened material, the only parameter altered in the model to predict the expansion of flyash specimen was the coefficient of diffusivity due to the major effects.

CONCLUSION

Sulfate resistance of two different flyash compositions was studied and compared with control specimens using ASTM C1012 standard prisms as well as modified size specimens. Expansion measurement was carried out in addition to Scanning Electron Microscopy (SEM) to study the microstructure of specimens affected by sulfate attack. It was observed that the general expansion behavior of cementitious systems could be obtained in a shorter period of time using modified specimens.

Application of a theoretical simulation model to predict the degradation due to external sulfate attack on cement-based materials was also discussed. A model based on series solution was presented and while the model uses a single diffusivity parameter, it is capable of predicting the test experimental test results using average properties. Simulation of the model using a series of parametric studies indicate that the effects of diffusivity of the material can play a significant role in the characteristics of sulfate penetration as well as w/cm ratio.

ACKNOWLEDGEMENT

We gratefully acknowledge the use of facilities within the Center for Solid State Science at Arizona State University. The authors would also like to appreciate the financial support of Salt River Project (SRP), and Salt River Materials Inc. in support of this project.

REFERENCES

[1] Skalny, J.; Marchand, J.; Odler, I., (2002) “Sulfate Attack on Concrete”, Spon Press, New York, NY, p. 43-126.

[2] Tixier, R., Mobasher, B., (2003) “Modeling of Damage in Cement–Based Materials Subjected To External Sulfate Attack- Part 1: Formulation”, *ASCE Journal of Materials Engineering*, 15 (4), p. 305-313.

[3] Standard Test Method for Length Change of Hydraulic Cement Mortars Exposed to a Sulfate Solution, ASTM C 1012-04 Vol. 04.01

[4] Clifton, J.R.; Frohnsdorff, G. and Ferraris, C. (1999) “Standards for Evaluating the Susceptibility of Cement Based Materials to External Sulfate Attack.” Materials Science of Concrete – Sulfate Attack Mechanisms, Special Volume, American Ceramic Society, p. 337-355.

[5] Ferraris, C.; Stutzman, P.; Peltz, M. and Winpigler, J. (2005) “Developing a More Rapid Test to Assess Sulfate Resistance of Hydraulic Cements.” Journal of Research of the National Institute of Standards and Technology, vol. 110, p. 529-540.

[6] Bentz, D.P. (2002). “Influence of Curing Conditions on Water Loss and Hydration in Cement Pastes with and without Flyash Substitution.” *NISTIR 6886*. Gaithersburg, MD, NIST.

[7] Philip, J. and Clifton, J.R (1992). “Concrete as an Engineered Alternative to Shallow Land Disposal of Low Level Nuclear Waste: Overview.” *Fly Ash, Silica Fume, Slag, and Natural Pozzolans in Concrete. Proceedings – Fourth International Conference*. Ed. V.M. Malhotra. Detroit: American Concrete Institute, vol. 1, p.713-730.

[8] Atkinson, A; Haxby, A. and Hearne, J.A. (1988) “The Chemistry and Expansion of Limestone-Portland Cement Mortars Exposed to Sulphate-Containing Solutions.” *NIREX Report NSS/R127*, United Kingdom: NIREX.

[9] Pommersheim, J.M., Clifton J.R (1994).”Expansion of Cementitious Materials Exposed to Sulfate Solutions.” *Scientific Basis for Nuclear Waste Management. Materials Research Society Symposium Proceedings XVII .* Ed.A. Barkatt and R. Van Konynenburg. Pittsburgh, Pa. : Materials Research Society, p. 363-368.

[10] Gospodinov, P., Kazandjiev, R., and Mironova, M. (1996). “Effect of Sulfate Ion Diffusion on the Structure of Cement Stone.” *Cement & Concrete Composites* 18 (6), p. 401-407.

[11] Gospodinov, P.N, Kazandjiev, R.F., Partalin, T.A. and Mironova, M.K.(1999). ”Diffusion of Sulfate Ions into Cement Stone Regarding Simultaneous Chemical Reactions and Resulting Effects.” *Cement and Concrete Research* 29 (10), p. 1591-1596.

[12] Krajcinovic, D, Basista, M., Mallick, K.and Sumarac, D(1992). “Chemo-Micromechanics Of Brittle Solids.” , *Journal of the Mechanics and Physics of Solids* 40 (5), p. 965-990.

[13] Tixier, R., Mobasher, B., (2003) “Modeling of Damage in Cement–Based Materials Subjected To External Sulfate Attack- Part 2: Comparison with Experiments”, *ASCE Journal of Materials Engineering*, 15 (4), p. 314-322.

[14] Mobasher, B., (2007) “Modeling of Stiffness Degradation and Expansion in Cement Based Materials Subjected to External Sulfate Attack.” , Materials Science of Concrete – Transport Properties and Concrete Quality, Special Volume, American Ceramic Society, p. 3157-171.